
INTELLIGENT4DSE: OPTIMIZING HIGH-LEVEL SYNTHESIS DESIGN SPACE EXPLORATION WITH GRAPH NEURAL NETWORKS AND LARGE LANGUAGE MODELS

Lei Xu, Shanshan Wang
Department of Computer Science
Shantou University
Shantou, China
{241xu, sswang}@stu.edu.cn

Emmanuel Casseau
IRISA
University of Rennes 1
Rennes, France
emmanuel.casseau@irisa.fr

Chenglong Xiao *
Department of Computer Science
Shantou University
Shantou, China
chl Xiao@stu.edu.cn

ABSTRACT

High-level synthesis (HLS) design space exploration (DSE) is an optimization process in electronic design automation (EDA) that systematically explores high-level design configurations to achieve Pareto-optimal hardware implementations balancing performance, area, and power (PPA). To optimize this process, HLS prediction tasks often employ message-passing neural networks (MPNNs), leveraging complex architectures to achieve high accuracy. These predictors serve as evaluators in the DSE process, effectively bypassing the time-consuming estimations traditionally required by HLS tools. However, existing models often prioritize structural complexity and minimization of training loss, overlooking task-specific characteristics. Additionally, while evolutionary algorithms are widely used in DSE, they typically require extensive domain-specific knowledge to design effective crossover and mutation operators. To address these limitations, we propose CoGNNs-LLMEA, a framework that integrates a graph neural network with task-adaptive message passing and a large language model-enhanced evolutionary algorithm. As a predictive model, CoGNNs directly leverages intermediate representations generated from source code after compiler front-end processing, enabling prediction of quality of results (QoR) without invoking HLS tools. Due to its strong adaptability to tasks, CoGNNs can be tuned to predict post-HLS and post-implementation outcomes, effectively bridging the gap between high-level abstractions and physical implementation characteristics. CoGNNs achieves state-of-the-art prediction accuracy in post-HLS QoR prediction, reducing mean prediction errors by $2.8\times$ for latency and $3.4\times$ for resource utilization compared to baseline models. For post-implementation prediction tasks, CoGNNs demonstrates the lowest prediction errors, with average reductions of 17.6% for flip-flop (FF) usage, 33.7% for critical path (CP) delay, 26.3% for power consumption, 38.3% for digital signal processor (DSP) utilization, and 40.8% for BRAM usage. Furthermore, LLMEA generates superior Pareto fronts compared to meta-heuristic algorithms simulated annealing algorithm (SA) and genetic algorithm (GA) demonstrating average distance from the reference set (ADRS) improvements of 89.5% and 86.0%, respectively.

Keywords High-Level Synthesis, Design Space Exploration, Graph Neural Networks, Large Language Models

1 Introduction

With the advancement of science and technology, improvements in chip performance are still heavily dependent on the integration scale of transistors. However, the limitations of Moore’s Law present formidable obstacles, making exponential growth in transistor integration increasingly difficult. As a result, this has spurred the demand for new computer architecture paradigms, such as domain-specific computing, leading to the rise of systems-on-chip (SoCs) at the chip level. These paradigms have further revolutionized traditional VLSI design methodologies, which historically relied on low-level hardware description languages such as Verilog or VHDL for meticulous RTL designs. HLS has

* *Corresponding Author:* **Chenglong Xiao.**

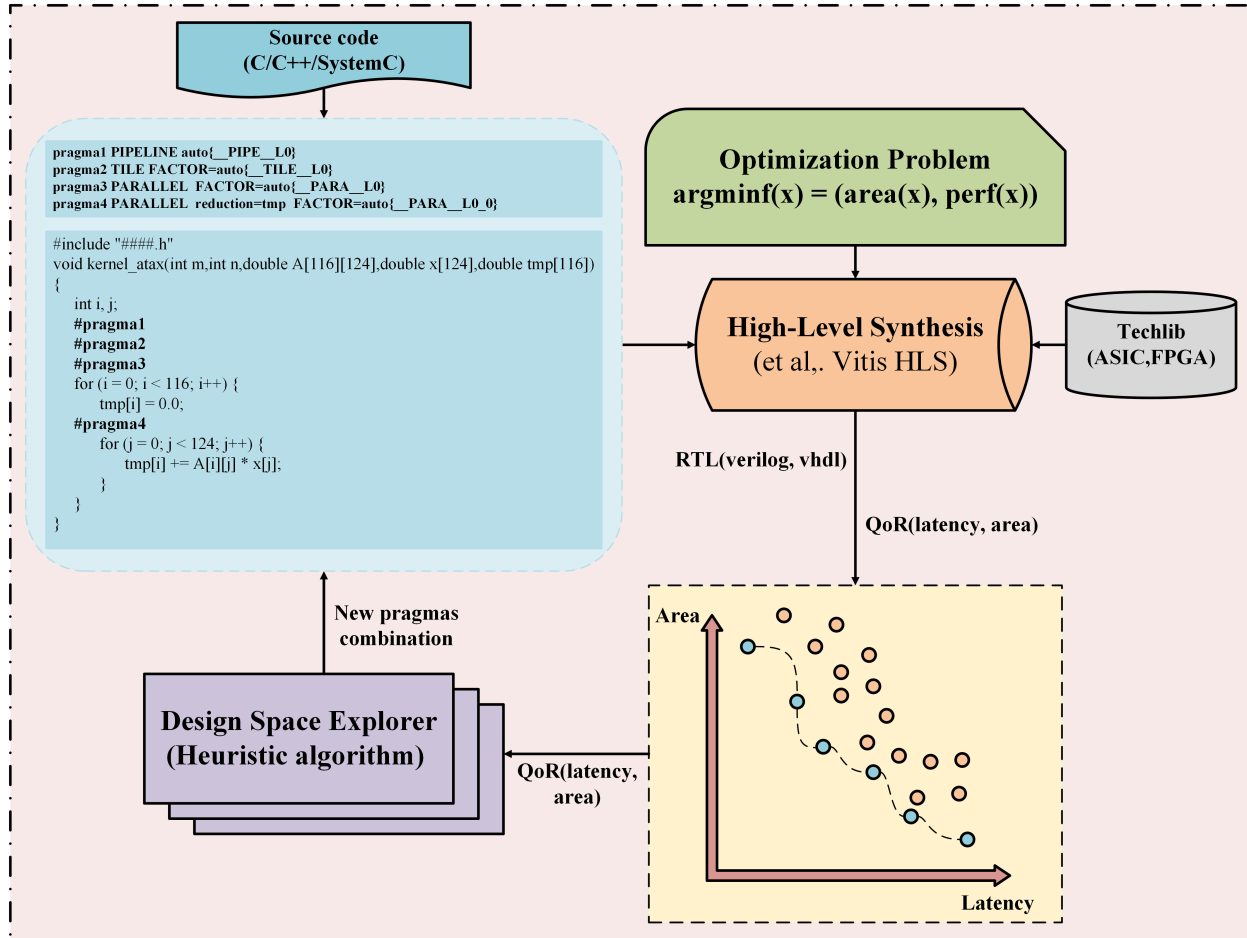


Figure 1: A comprehensive overview of the HLS DSE process, using the atax application from the PolyBench benchmark suite. The HLS tool can be replaced by predictive models.

emerged as a modern alternative to traditional RTL-based VLSI design. HLS enables users to leverage high-level programming languages, such as C/C++, for hardware design tasks, offering synthesis options to fine-tune results. Proven in practice, HLS provides numerous advantages in hardware design and has become the mainstream approach, particularly for FPGA implementations. To enhance HLS effectiveness, most EDA tools offer a variety of synthesis options, called "knobs," allowing users to control the synthesis outcomes. In commercial HLS tools, synthesis directives are typically added to the source code as comments or pragmas.

As illustrated in Figure 1, this work presents a systematic framework for HLS DSE. The workflow begins with C/C++ behavioral descriptions augmented with pragma directives and parameterized optimization targets. These specifications are synthesized using HLS tools to generate QoR metrics (e.g., latency, resource utilization). A design space exploration engine then selects novel pragma combinations through multi-objective optimization, generating updated behavioral descriptions for subsequent iterations. This cyclic refinement process continues until the convergence to a Pareto-optimal configuration set that optimally balances competing design constraints. However, evaluating the performance of each design configuration using HLS tools can be time-consuming, especially when excessive pragmas are inserted, leading to prolonged synthesis times. The pragma directives exhibit non-unique value assignments, leading to a combinatorial explosion of design configurations (e.g., loop unrolling factors, array partitioning schemes) that must be explored during HLS optimization [1]. Given the high computational cost of HLS tool evaluations, providing the quality of results for each combination in the design space would require an impractical amount of time. Thus, for HLS DSE, it is crucial to efficiently predict the results such as latency and resource utilization for each design combination and identify the optimal configurations within the vast design space.

Graph neural networks (GNNs) based on the message-passing mechanism, commonly termed MPNNs, operate by iteratively updating node features through neighborhood information aggregation. Although these MPNNs demonstrate strong accuracy in conventional classification and regression tasks, their performance in HLS QoR prediction tasks

remains limited, often failing to surpass the discriminative power of the 1-Weisfeiler-Lehman (1-WL) algorithm [2]. This limitation comes from their restricted expressiveness, leading to sub-optimal performance in complex prediction tasks. Xu et al. [3] theoretically established that MPNNs' expressive capacity is bounded by the 1-WL test. Furthermore, MPNNs face two critical challenges:

- 1) Long-range dependency issues [4]: Traditional MPNNs update node features by aggregating local neighbor information, effectively capturing direct connections but struggling to model interactions between distant nodes. This shortcoming significantly impacts tasks requiring global topological awareness.
- 2) Over-smoothing phenomena [5]: As network depth increases, repeated neighborhood aggregation causes node representations to converge toward indistinguishable states, severely degrading performance in multi-target prediction scenarios.

DSE methods systematically explore the design space to identify Pareto-optimal configurations that achieve optimal trade-offs between competing objectives such as performance and cost. A Pareto-optimal design is defined as one that exhibits both reduced area and lower latency compared to all other feasible solutions within the search space, such that no further improvement can be made in either metric without degrading the other. However, conventional DSE approaches face two critical limitations:

- 1) They are prone to converging to local optima due to insufficient global search capabilities.
- 2) Existing DSE optimization algorithms such as genetic algorithm (GA) and simulated annealing (SA) suffer from demanding parameter tuning requirements. Traditional evolutionary approaches not only require domain-specific knowledge to design sophisticated crossover and mutation operators but also involve computationally intensive parameter optimization processes that consume substantial time and resources during evolutionary computation.

In this work, we employ CoGNNs [2] — a novel graph neural network architecture with an adaptive message-passing mechanism as our core prediction model. Compared to traditional GNN paradigms, CoGNNs exhibits three key innovations:

- 1) **Task-Specific Adaptivity:** While conventional message-passing mechanisms uniformly aggregate neighbor information through fixed computational graphs, CoGNNs dynamically reconstructs the graph topology based on task objectives, enabling targeted feature propagation.
- 2) **Training Efficiency:** Unlike baseline models requiring extensive training iterations to learn optimal aggregation weights (e.g., graph attention network's attention coefficients [6]), CoGNNs achieves comparable performance with significantly fewer training cycles by optimizing computational graph structures.
- 3) **Over-Smoothing Mitigation:** Traditional MPNNs suffer from feature homogenization in deep layers due to repetitive neighborhood aggregation. CoGNNs addresses this by implementing layer-wise heterogeneous graph topologies, thereby effectively mitigating node representation degeneration.

Furthermore, we integrate large language models (LLMs) to enhance EA (Evolutionary Algorithms). Capitalizing on LLMs' exceptional capabilities in code synthesis and semantic reasoning, we redesign EA operators through carefully engineered prompts. This hybrid approach reduces exploration costs while improving solution quality through synergistic human-AI collaboration. In summary, our work makes the following key contributions:

- **Task-Adaptive Graph Neural Framework:** We present an enhanced CoGNNs framework that introduces two critical modifications to address the limitations of conventional MPNNs: a dynamic topology reconstruction mechanism enabling task-specific graph adaptation and layer-wise heterogeneous message passing to mitigate feature homogenization in deep architectures.
- **Progressive Prediction Strategy:** To rigorously assess the predictive model's cross-abstraction accuracy, we expand our validation framework by integrating implementation report-derived datasets alongside conventional HLS report-based benchmarks. This multi-fidelity evaluation methodology demonstrates CoGNNs' capability to maintain precision across distinct hardware abstraction levels from high-level synthesis metrics (e.g., estimated latency) to post-implementation physical characteristics (e.g., placed-and-routed resource utilization) while preserving its task-adaptive message passing architecture.
- **LLM-Enhanced Evolutionary Exploration:** We develop LLMEA, the first evolutionary algorithm that integrates large language models for HLS DSE. By leveraging LLMs' reasoning capabilities with carefully engineered prompts, LLMEA reduces domain expertise dependency and achieves prominent improvement in Pareto front quality compared to baseline algorithms.

2 Related work

Recent advances in QoR prediction have been driven by machine learning and GNNs. Foundational approaches employ learnable parameters and loss minimization to predict optimal configurations, with notable contributions including systematic regression model analysis for HLS feature selection [7] and accelerator evaluation framework MPSeeker [8]. Makrani et al. [9] employ Minerva, an automated hardware optimization tool that determines near-optimal tool configurations through static timing analysis and heuristic algorithms, optimizing either peak throughput or throughput-to-area ratio. Pyramid framework leverages this database to train an ensemble ML model that maps HLS-reported features to Minerva’s optimization outcomes. Building on these foundations, GNN-based methods have emerged as the dominant paradigm, typically converting source code into intermediate representation (IR) graphs for feature extraction exemplified by hybrid control-dataflow graphs [10] and hierarchy-aware GNNs [11]. Recent studies demonstrate progressive advancements in GNN-based hardware design optimization. Wu et al. [12] develop performance modeling frameworks using graph neural networks to represent C/C++ programs as computational graphs. Extending this paradigm, Zhao et al. [13] establish GNNHLS as an HLS-specific benchmark with six GNN models across four topological datasets. While Lin et al. [14] propose power-aware edge-centric GNNs with dynamic power modeling through edge neighborhood aggregation, Kuang et al. [15] introduce hierarchical HGP architectures for post-implementation PPA prediction. Complementing these approaches, Sohrabizadeh et al. [16] present HARP’s hierarchical graph representation with auxiliary nodes for pragma-optimized HLS designs.

DSE is fundamentally formulated as a multi-objective optimization problem (MOOP), where pre-trained prediction models can serve as evaluators to guide heuristic search algorithms toward Pareto-optimal solutions. Recent research in design space exploration integrates diverse machine learning paradigms with optimization frameworks. Wang et al. [17] automate meta-heuristic parameter configuration through behavioral analysis of C-based descriptions, while Goswami et al. [18] demonstrate GBRT-based models achieve comparable accuracy to exhaustive logic synthesis. For enabling precise identification of Pareto-optimal designs, Hong et al. [19] develop contrastive learning for predicting the dominance relationships between designs. A reinforcement learning driven DSE approach is presented in [20]. Yao et al. [21] propose a decomposition based DSE approach to minimize synthesis iterations. To accelerate ASIC DSE, Rashid et al. [22] introduce FPGA-targeted transfer learning and a dedicated multithreaded parallel HLS design space explorer. Zou et al. [23] propose FlexWalker, a multi-objective HLS design space exploration framework that employs upper confidence bound (UCB)-coordinated heterogeneous regression models for design quality prediction across parameter configurations, augmented with probabilistic sampling and elastic Pareto frontiers to mitigate regression modeling inaccuracies.

In summary, SOTA prediction methodologies in HLS primarily depend on GNNs, leveraging their inference capabilities to achieve high-precision predictions on unseen datasets. Dominant GNN architectures including Graph Convolutional Networks (GCNs) [24], Graph Attention Networks (GATs) [6], and Graph Isomorphism Networks (GINs) [3] are rooted in message-passing mechanisms. However, inherent limitations of MPNNs, such as long-range dependency failures and over-smoothing phenomena, critically degrade prediction accuracy, partially explaining the persistent performance gaps in HLS QoR estimation. For DSE, heuristic algorithms such as GA and SA remain widely adopted. While EAs demonstrate exceptional competence in addressing multi-objective optimization challenges via evolutionary operators, traditional implementations are constrained by two fundamental limitations: excessive dependency on manual hyperparameter configuration and premature convergence phenomena to local optima resulting from compromised global search capabilities. These limitations underscore the need for adaptive EA frameworks capable of balancing exploitation and exploration.

3 Preliminaries

3.1 Program Graph Representation with Multi-Aspect Embeddings

To facilitate GNNs in capturing the features of the source code, we construct hierarchical graph representations that preserve both syntactic structures and semantic dependencies. A prevalent approach nowadays is to use LLVM [25] to convert the source code into IR, and then utilize ProGraML [26] to transform the IR into a control data flow graph. LLVM instructions encompass numerous low-level operations such as addition operations and memory reading operations. These operations are converted into certain nodes in the control data flow graph (CDFG). If an operation needs to be performed on a certain variable, the corresponding nodes will be connected through some directed edges.

3.2 Graph Neural Network

A simple graph neural network extracts the features of each node during the training process and aggregates the messages from its neighbors to update the node features. Specifically, at GNN’s l -th layer, node v ’s feature representation h_v^l

will be updated by aggregating (*AGG*) node v 's feature representation h_v^{l-1} in the previous layer and all the neighbor messages h_w^{l-1} , where $w \in N(v)$ and $N(v)$ is a neighbor set of node v . To make this process learnable, the result obtained above needs to be multiplied by the learnable weight matrix W^{l-1} .

$$h_v^l = \sigma(W^{l-1}h_v^{l-1} + W^l\psi(h_w^{l-1}, \forall w \in N(v))) \quad (1)$$

where σ is a *activation* function to provide non-linearity and ψ is *aggregation* function like *mean*, W^{l-1} and W^l are learnable matrices.

3.3 Evolutionary Algorithms for HLS DSE

In HLS DSE, GAs [17] are widely adopted as the optimization backbone, where each design configuration is encoded as a gene and the complete set forms a chromosome C_r . The exploration begins with an initial population of parent configurations, which undergo crossover and mutation operations guided by predefined probabilities to generate offspring by modifying pragma values (e.g., loop unrolling factors, array partitioning schemes). Recent advancements [8]-[15] have integrated prediction models as evaluators, replacing computationally expensive commercial HLS tools. This hybrid approach synthesizes the current population (parents + offspring) using the prediction model to estimate latency and resource utilization, retains configurations with superior Pareto-optimal trade-offs, and halts when predefined conditions are met.

3.4 Gumbel-softmax Estimator

In CoGNNs, the action network dynamically adjusts the node states based on task-specific characteristics, enabling adaptive reconstruction of the computational graph topology. Specifically, the action network performs a node-level classification task to predict discrete state assignments, where the optimal state is selected via argmax over the predicted probabilities. However, since node states follow a categorical distribution, this prediction task is inherently non-differentiable. To address this, CoGNNs employ the Gumbel-Softmax estimator [27], which provides a continuous relaxation of the discrete state selection process, thereby enabling end-to-end gradient-based optimization. This approach ensures both the dynamic adaptability of the graph structure and the trainability of the overall framework. This estimator approximates the stochastic action sampling in a differentiable and continuous manner. We consider a set of actions Υ , which can be represented as a probability vector $p \in \mathbb{R}^{|\Upsilon|}$ and the vector p stores the probability values of different actions. Let q be a categorical variable with class probabilities $p_1, p_2, \dots, p_{|\Upsilon|}$ and we assume that the categorical samples are encoded as k-dimensional one-hot vectors. The Gumbel-Max is a special reparametrization trick that provides an efficient way to draw samples q from a categorical distribution with class probabilities p :

$$q = \text{onehot} \left(\underset{k}{\operatorname{argmax}} (g_k + \log p_k) \right) \quad (2)$$

where $g_1, g_2, \dots, g_{|\Upsilon|}$ are samples drawn from Gumbel(0, 1). We can use the softmax function to replace the non-differentiable argmax function to generate the Gumbel-softmax scores s_k and τ is the softmax temperature:

$$s_k = \frac{\exp((g_k + \log p_k) / \tau)}{\sum_{i=1}^{|\Upsilon|} \exp((g_i + \log p_i) / \tau)} \quad (3)$$

By incorporating the Gumbel-Softmax estimator, the action network becomes fully differentiable, enabling its seamless integration into the gradient-based optimization process. This differentiability allows CoGNNs to dynamically adapt node-level actions such as edge pruning or feature aggregation based on task-specific objectives. Consequently, the framework learns data graph features in a topology-aware manner, capturing both local structural patterns and global semantic dependencies. This adaptive capability is particularly advantageous for HLS prediction tasks, where design configurations exhibit heterogeneous and hierarchical characteristics.

3.5 Problem Formulation

HLS DSE can be formulated as a MOOP, where the primary objective is to identify a set of Pareto-optimal configurations that simultaneously minimize latency and resource utilization. Given a behavioral description and optional synthesis directives [$\text{pragma}_1, \text{pragma}_2, \dots, \text{pragma}_n$], the design space DS can be formulated as the Cartesian product of the combination of pragmas. The definition of Pareto frontier P_f is as follows [1]:

$$A(d_f) \leq A(d_i) \text{ and } L(d_f) \leq L(d_i) \quad (4)$$

where $d_f \in P_f$, $d_i \in DS$ and $P_f \subseteq DS$. The function $A(\cdot)$ and $L(\cdot)$ represent the resource utilization and the latency of d_f and d_i . A design configuration $d_j \in P_f$ is considered Pareto-optimal if no other configuration in the search space

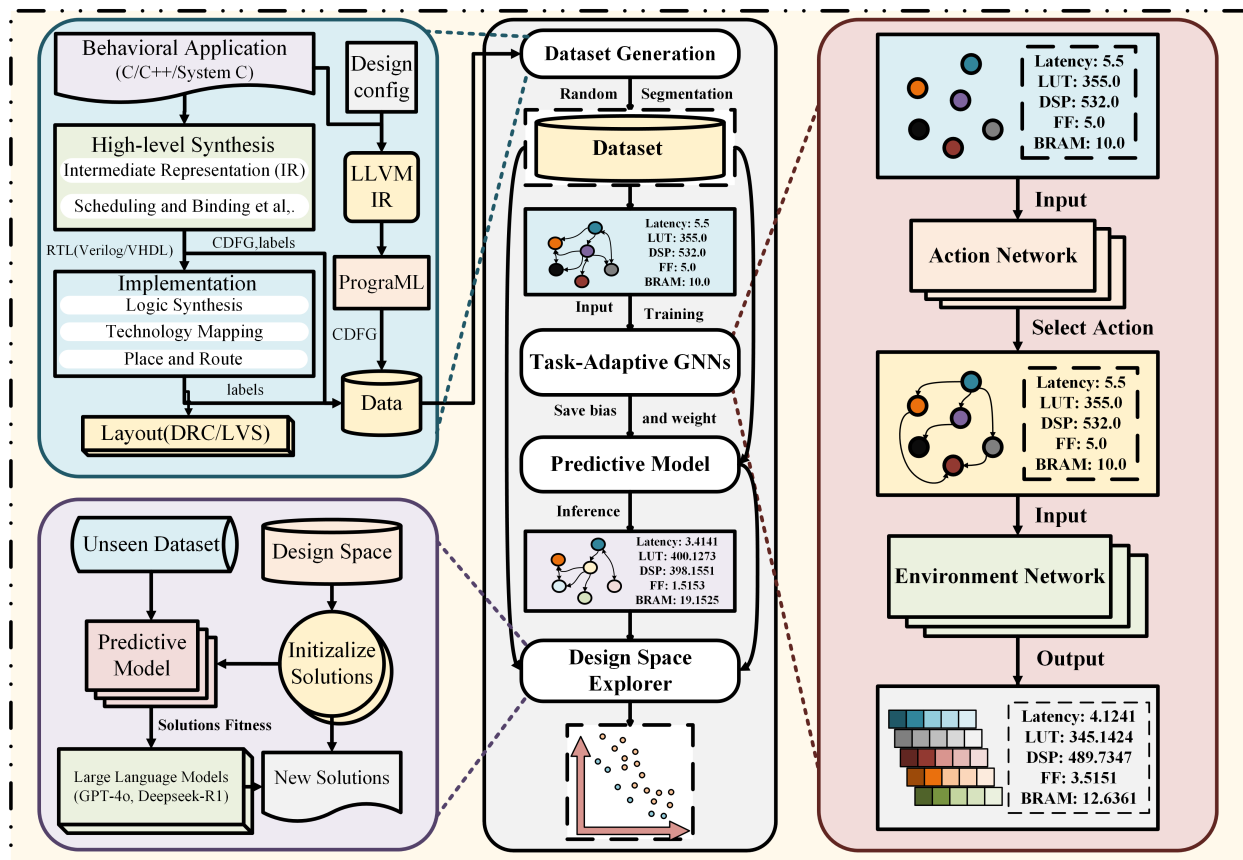


Figure 2: The CoGNNs-LLMEA framework integrates data generation (combining HLS reports and implementation reports), predictive model training via task-adaptive graph neural networks, and DSE using an LLM-enhanced evolutionary algorithm. The CoGNNs can be tuned to predict post-HLS QoR metrics and post-implementation QoR metrics.

dominates it, that is, no alternative design simultaneously achieves both lower area utilization and reduced latency. Therefore, our objective is to efficiently identify the Pareto-optimal set without resorting to exhaustive searches across the entire configuration space and invoking computationally expensive HLS tools.

4 Methodology

Figure 2 provides an overview of the proposed CoGNNs-LLMEA. The proposed framework integrates four key stages: dataset generation, model training, inference, and DSE. During dataset generation, labels are extracted from both HLS reports (e.g., loop initiation intervals, resource estimates) and implementation reports (e.g., post-place-and-route resource usage, timing closure) to enhance prediction accuracy. For model training, a subset of the dataset is used to train CoGNNs composed of an environment network (global context capture), an action network (dynamic topology adjustment), and a multi-layer perceptron (QoR metric mapping) which iteratively improves prediction accuracy through hierarchical feature extraction. In the inference stage, the trained CoGNNs model predicts QoR metrics for unseen configurations, enabling rapid evaluation without invocations of the HLS tool. Finally, the DSE stage employs a modified evolutionary algorithms enhanced by LLMs to identify near-Pareto-optimal solutions.

4.1 Dataset Generation

The C/C++ source code is first converted to an intermediate representation (IR) using LLVM, followed by the generation of a CDFG through ProGraML [26], which incorporates HLS directives for enhanced semantic representation. The CDFG generated through this compilation process serves as the foundational input to the CoGNNs prediction model. Each design configuration is then synthesized using an HLS tool to extract latency and resource utilization metrics. Although HLS reports provide reasonably accurate estimates, we further refine the dataset by incorporating post-implementation metrics, resulting in a more realistic and comprehensive training set. This dual-source labeling strategy

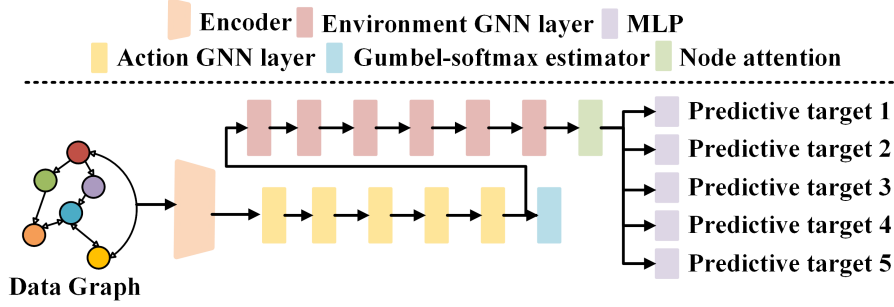


Figure 3: An abstract illustration of the CoGNNs architecture, where a dedicated MLP is constructed for each prediction target.

combining HLS and implementation reports ensures high-fidelity ground truth for model training. We train our prediction model on datasets from [15] and [28]. For the GNN-DSE dataset [28], the labels for each benchmark are extracted from the HLS reports, and the CFGs are generated by the compilation front-end. For the HGBO-DSE dataset [15], the labels are derived from the implementation reports, and the CFGs come from the HLS process. The two aforementioned datasets differ not only in their label sources but also in the benchmarks used for their construction. By conducting experiments on two distinct datasets, we can comprehensively validate the performance of CoGNNs and evaluate its efficiency in handling complex tasks.

4.2 Cooperative Graph Neural Networks

CoGNNs [2] introduces a dynamic message-passing mechanism by assigning each node one of four states — Standard (S), Listen (L), Broadcast (B), or Isolate (I), which govern information flow: nodes in the Standard state both receive and propagate information, Listen nodes only receive, Broadcast nodes only propagate, and Isolate nodes remain inactive. This state-based approach transforms node feature updates into a two-step process: 1) each node selects its optimal state based on task-specific objectives, and 2) updates its features accordingly. As illustrated in Figure 3, CoGNNs implements this mechanism through dual MPNNs: an action network that determines node states and an environment network that performs context-aware feature aggregation.

A complete CoGNN (π, η) model consists of environment networks π and action networks η . These two MPNNs, working in tandem, can better adapt to multi-target prediction tasks. Action networks π help each node determine the way information flows in and out, while environment networks η update the features of each node according to the state of the node. Therefore, CoGNNs update the feature representation h_v of each node v according to the following steps. To begin with, the action networks π will obtain the action of each node. For a set of actions $\Phi = \{S, L, B, I\}$, the action of node v can be drawn from a categorical distribution $p_v \in \mathbb{R}^{|\Phi|}$ by aggregating the information of its neighbors $N(v)$.

$$p_v = \pi(h_v, N(v)) \quad (5)$$

Next, we input the probability vector p_v into the Gumbel-softmax Estimator to obtain the action of the node a_v . We can use environment networks η to update the feature representation h_v and obtain h'_v .

$$h'_v = \eta(h_v, \mathcal{N}) \quad (6)$$

where \mathcal{N} is related to the value of a_v :

$$\mathcal{N} = \begin{cases} \{h_u | u \in N(v), a_u = S \vee B\}, & a_v = L \vee S \\ \{\}, & a_v = B \vee I \end{cases} \quad (7)$$

For the environment and action networks, we employ a combination of aggregation models (e.g., MEANGNN, SUMGNN) to iteratively update node feature representations. To construct the graph-level embedding, we replace CoGNNs' direct node feature summation with an attention-based mechanism [29], which assigns importance scores t_v to each node v based on its relevance to the HLS prediction task. This approach captures the heterogeneous contributions of nodes (e.g., loop headers vs. memory operations) and computes the final graph-level vector h_G by weighted summation.

$$h_G = \sum_{i=1}^n \left(\frac{\exp^{MLP_1(h_i)}}{\sum_{j=1}^n \exp^{MLP_1(h_j)}} \right) \times MLP_2(h_i) \quad (8)$$

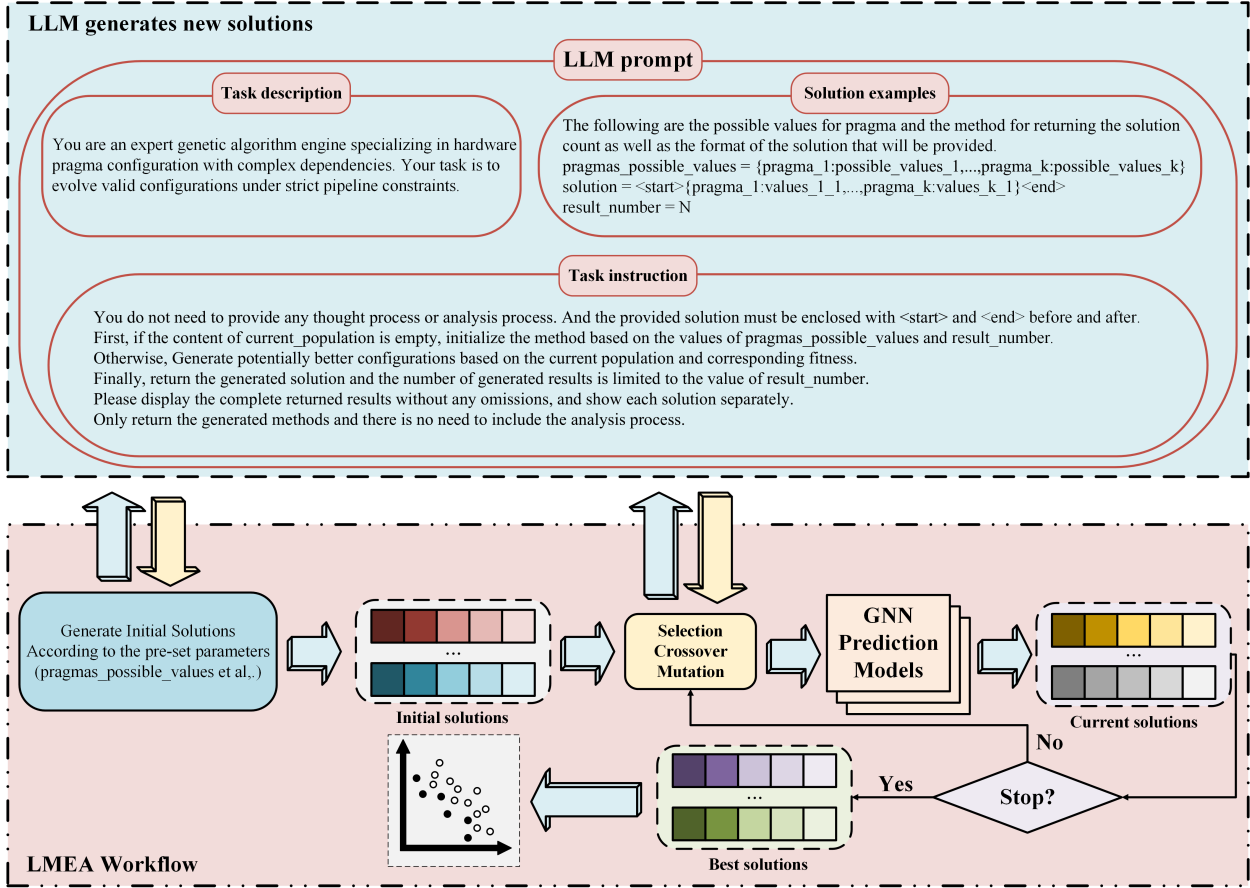


Figure 4: The LLMEA framework integrates prompt design (comprising task description, solution examples, and task instructions) and an LLM-enhanced workflow (including initialization, LLM-guided solution generation, and GNN-based evaluation).

where n is the total number of nodes in the data graph, and MLP_1 and MLP_2 are used to map h_i and h_j to \mathbb{R} . In the prediction phase, we set up MLPs for each prediction target. Compared to [15], this method only requires training one prediction model to predict all targets.

4.3 Large Language Model aided Evolutionary Algorithms

Traditional heuristic algorithms, such as EAs, have demonstrated strong performance in DSE. However, EAs often require extensive domain expertise to carefully design selection, crossover, and mutation operators, which may lead to suboptimal solutions due to premature convergence to local optima. To address this limitation, we leverage large language models (LLMs) to assist EAs in generating offspring through selection, crossover, and mutation. Li et al. [30] highlighted the importance of well-designed prompts to guide LLMs in generating offspring, while Meyerson et al. [31] demonstrated that Few-Shot Prompting can effectively instruct LLMs to improve the crossover and mutation processes, yielding superior results. As illustrated in Figure 4, we design prompts tailored to the dataset characteristics and incorporate the Few-Shot method to guide the LLM in performing selection, crossover and mutation.

The lower section of the figure 4 depicts the main process of the evolutionary algorithm for DSE, while the upper section of the figure illustrates the prompt structure. LangChain², an open-source framework, facilitates the development of applications utilizing LLMs by offering tools, components, and interfaces for integrating LLMs with external data sources and services. We employ LangChain to configure our LLMs, necessitating prompt designs that adhere to its format. The prompts are categorized into system messages and input messages. The system messages inform the LLMs about the task’s content and requirements, while the input messages transmit data for each LLM API call. Within the system messages, we design two sections: scenario introduction, method examples, and task description. The scenario introduction instructs the LLM to assume the role of an expert in evolutionary computing, enabling it to leverage relevant knowledge without explicit details about the genetic algorithm process. The task description section comprises

²<https://github.com/langchain-ai/langchain>

Algorithm 1 The DSE algorithm–LLMEA framework.

Input: Design space DS , design space size S , pragma possible values V_p , maximal iterations N_{se} , population size N , graph code $code$;

Output: Pareto optimal solution set P_{est} ;

```

1:  $n = 1$ ;
2: while  $n \leq N_{se}$  do
3:   if  $n == 1$  then
4:      $prompts \leftarrow$  based on  $N, V_p$  to establish LLM prompt;
5:      $P \leftarrow$  use  $prompts$  to instruct LLM to initialize  $N$  solutions;
6:   else
7:      $prompts \leftarrow$  based on  $N, V_p, Fitness$  to establish LLM prompt;
8:      $P_{new} \leftarrow$  use  $prompts$  to instruct LLM to generate new offspring solutions.
9:   end if
10:   $P, Fitness \leftarrow$  Selector( $P, P_{new}, code$ )
11:   $n \leftarrow n + 1$ 
12: end while
13:  $P_{est} \leftarrow$  the best solutions in  $P$ 
14: return  $P_{est}$ 

```

inputs, outputs, and instructions. The inputs and outputs specify the information the LLMs should collect and generate, respectively, while the instructions detail how the LLMs should process the inputs. Since LangChain is used to invoke the LLM API, the input messages are designed to include only parameters relevant to the design space.

Algorithm 1 provides an overview of the LLMEA framework. The inputs of the algorithm include the parameters required for LLM prompts and those related to the design space, while the output is the Pareto-optimal set P_{est} . A conditional statement determines whether to instruct the LLMs to generate an initial population based on the provided prompts or to produce potentially improved solutions based on the current population and fitness scores (lines 3-9). The exploration engine employs the pre-trained predictive models to assess the $Fitness$ of each new solution in the current population and selects top N configurations, updating both the current population P and returning the fitness of population $Fitness$ (line 10). The fitness is primarily composed of two key metrics: estimated latency derived from critical path analysis and resource utilization metrics including LUT, DSP, FF and BRAM usage. This process repeats until the loop terminates, at which point the solutions in P are added to P_{est} , and the Pareto-optimal solution set P_{est} is returned (lines 13–14).

5 Experiments

5.1 Experimental Setup

In the experiments, the datasets are sourced from SOTA works GNN-DSE [28] and HGBO-DSE [15]. The GNN-DSE dataset, containing latency and resource usage labels, is extracted from HLS reports, while the HGBO-DSE dataset with PPA results is derived from post-implementation reports. Since the proposed method can be used for predicting both the post-HLS QoRs and the post-implementation QoRs, we compare it with SOTA works on the aforementioned two datasets respectively. To evaluate the proposed DSE algorithm, we use the most accurate prediction model based on experimental evaluation as the estimator for DSE, which collaborates with LLMEA in Section 4.3 to ultimately obtain the Pareto-optimal solution set. The applications in the GNN-DSE dataset are sourced from MachSuite [32] and Polyhedral [33] benchmarks, which involve 7 applications for training, testing, and validation and 5 for DSE exploration, while the HGBO-DSE dataset includes 10 applications from MachSuite, with 6 for training, testing, and validation and 4 for inference. The experiments are conducted on the AMD Ultrascale+ MPSoC ZCU104. The benchmarks are synthesized using Vitis-HLS 2022.1 and Vivado 2022.1 to collect ground-truth latency and resource utilization metrics, which serve as training labels for the model.

Both datasets are randomly divided into 70% for training, 15% for testing, and 15% for validation. In the experiments, CoGNNs’ environment network has three layers and the action network has two layers, with MEANGNN, SUMGNN, and GCN as the main GNN types selectable for both networks, from which the most suitable combination for the QoR prediction task is chosen. Meanwhile, the hidden layer dimension of all models is set to 128, and the Adam optimizer is used, with the GNN-DSE dataset experiments use a batch size of 64, a learning rate of 0.001, and over 500 iterations, while the HGBO-DSE dataset experiments employing a batch size of 128, a learning rate of 0.001, and over 250 iterations. To be consistent with GNN-DSE [28] and HGBO-DSE [15], Root Mean Squared Error (RMSE) loss is used

Table 1: The training applications used for post-HLS QoR prediction.

Kernel name	Description	# Pragmas	# Design configs
<i>aes</i>	a common block cipher	3	45
<i>gemm-blocked</i>	A blocked version of matrix multiplication	9	2,314
<i>gemm-ncubed</i>	O(n3) algorithm for dense matrix multiplication.	7	7,792
<i>nw</i>	A dynamic programming algorithm for optimal sequence alignment	6	15,288
<i>spmv-crs</i>	Sparse matrix-vector multiplication, using variable-length neighbor lists	3	114
<i>spmv-ellpack</i>	Sparse matrix-vector multiplication, using fixed-size neighbor lists	3	114
<i>stencil3d</i>	A three-dimensional stencil computation	7	7,591

Table 2: RMSE loss of different CoGNNs on unseen applications. The top models are marked in bold.

Model	Latency	LUT	DSP	FF	BRAM	All
CoGNNs(α, α)	0.4315	0.0043	0.0114	0.0155	0.0270	0.4897
CoGNNs(α, β)	0.7101	0.0084	0.0141	0.0279	0.0333	0.7937
CoGNNs(β, β)	0.5077	0.0053	0.0091	0.0146	0.0353	0.5720
CoGNNs(β, α)	0.3557	0.0039	0.0075	0.0152	0.0244	0.4067
CoGNNs(γ, β)	0.6748	0.0067	0.0167	0.0229	0.0331	0.7541
CoGNNs(γ, γ)	0.5825	0.0063	0.0126	0.0252	0.0324	0.6592
CoGNNs(α, γ)	0.4131	0.0174	0.0276	0.1193	0.0297	0.6072
CoGNNs(β, γ)	0.6456	0.0112	0.0248	0.0434	0.0346	0.7596

to quantify the post-HLS QoR prediction quality, and Mean Absolute Error (MAE) and Mean Absolute Percentage Error (MAPE) are used to evaluate the accuracy of the models for the post-implementation QoR prediction. The CoGNNs model proposed in this paper, along with the baseline models and the DSE algorithms, are all implemented in Python.

5.2 Evaluation of Post-HLS QoR Prediction Accuracy

In this experiment, to validate the prediction accuracy of CoGNNs for estimating post-HLS QoR metrics, we leverage the architectural flexibility of CoGNNs to design eight combinations of environment and action networks for predicting latency, LUT, DSP, FF and BRAM usage, comparing their performance against baseline models. For clarity, we denote MEANGNNs [34], SUMGNNs [34], and GCN [24] as α , β , γ , respectively, to describe different CoGNNs configurations. The SUMGNNs and MEANGNNs mentioned here are two fundamental variants of MPNNs that differ in their neighborhood aggregation functions, with SUMGNNs using summation-based aggregation and MEANGNNs employing mean-based aggregation. Additionally, we evaluate baseline models including GNN-DSE [28], HGP+SAGE+GF [15], IronMan-Pro [20], PNA-R [12], and PowerGear [14]. While PNA-R and PowerGear are primarily designed for post-implementation prediction tasks (PowerGear proposes GNN to predict power), we adapt these baseline models for post-HLS scenarios by modifying their input dimensions to align with the feature space of the GNN-DSE dataset and restructuring their architectures using the PyTorch Geometric framework. These adaptations enable competitive performance in post-HLS prediction tasks, demonstrating the models’ flexibility across different hardware abstraction levels. As shown in Table 1, the HLS prediction dataset primarily comprises benchmarks such as *aes* and *gemm-blocked*. GNN-DSE [28] employs a Redis-based service to implement an online dataset provisioning mechanism, ensuring strict separation between training and inference datasets while maintaining benchmark diversity across both data splits.

As shown in Table 2, we conducted extensive experiments on this dataset and recorded the RMSE of models. RMSE is squared-error metric measuring prediction accuracy via root-averaged discrepancies between predicted and actual values, preserving data units. For latency prediction, CoGNNs(β, α) achieves the best performance, followed by CoGNNs(α, γ) with prediction errors of 0.3557 and 0.4131, respectively. In contrast, CoGNNs predicts multiple targets within an integrated framework, achieving high accuracy overall. For DSP and FF resource prediction, CoGNNs(β, α) and CoGNNs(β, β) deliver the best results. For the prediction of LUT and BRAM, CoGNNs(β, α) and CoGNNs(β, β) achieve the smallest prediction errors. Although CoGNNs(β, α) has a slightly higher prediction error (0.0006) than CoGNNs(β, β) in FF prediction, its overall error is 0.083 lower than CoGNNs(α, α). Thus, we conclude that CoGNNs(β, α) exhibits the best CoGNNs combination on the GNN-DSE dataset. As empirically validated in Figure

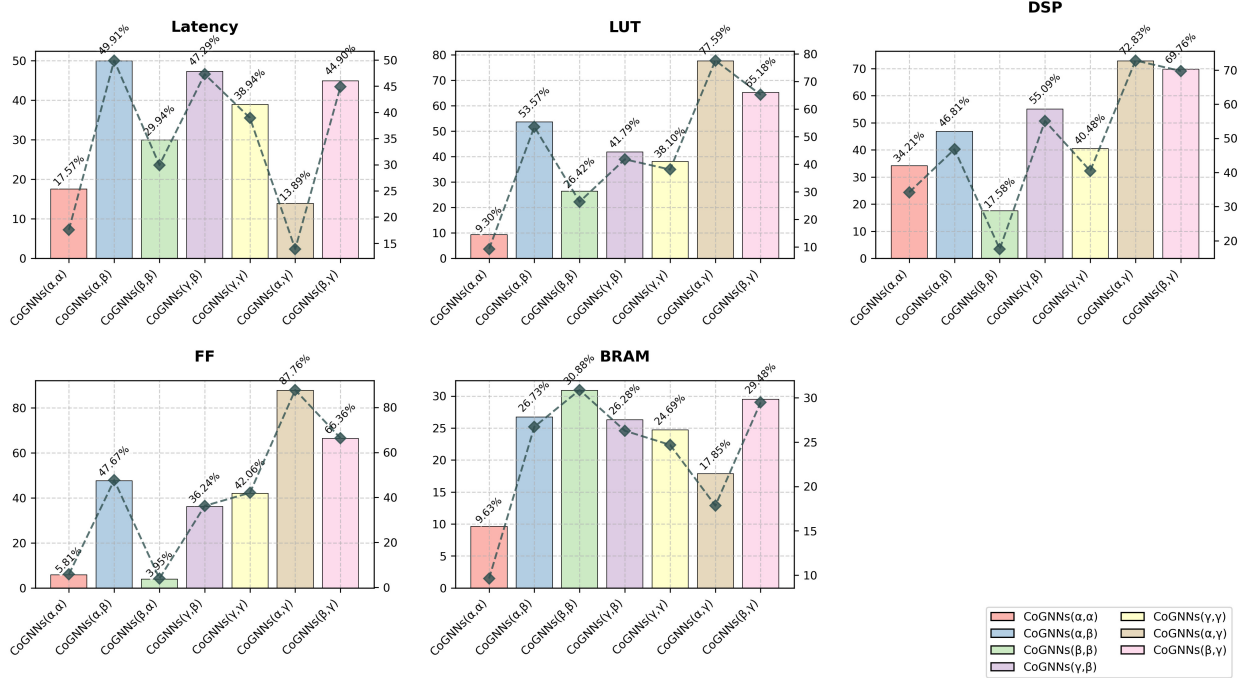


Figure 5: Reduction rates of RMSE loss achieved by CoGNNs(β, α) over other CoGNNs (For FF, we present the reduction rates of RMSE loss achieved by CoGNNs(β, β) over other CoGNNs). The bar chart quantifies each model’s prediction error reduction ratios (PERR) relative to the top-performing model, while the line chart tracks the evolving PERR trend across evaluation metrics.

Table 3: RMSE loss of CoGNNs(β, α) and SOTA models on unseen applications. The top models are marked in bold.

Model	Latency	LUT	DSP	FF	BRAM	All
GNN-DSE[28]	0.5359	0.0762	0.1253	0.0632	0.0515	0.8521
HGP+SAGE+GF[15]	0.9519	0.0152	0.0270	0.0895	0.0362	1.1197
IronMan-Pro[20]	0.6778	0.0081	0.0161	0.0399	0.0326	0.7745
PNA-R[12]	1.3728	0.0144	0.0307	0.0811	0.0610	1.5600
PowerGear[14]	1.3956	0.0177	0.0290	0.0908	0.0432	1.5764
CoGNNs(β, α)	0.3557	0.0039	0.0075	0.0152	0.0244	0.4067

5, the CoGNN(β, α) demonstrates statistically significant error reduction across multiple prediction targets when compared with other configurations of CoGNNs. In comparison with other combination, CoGNN(β, α) demonstrates statistically significant reductions in prediction errors across all metrics except FF prediction targets. Specifically regarding the Latency metric, CoGNN(β, α) achieves a minimum RMSE reduction ratio of 13.89%. For DSP indicators, the maximum prediction error reduction reaches 72.83% when using CoGNNs. Notably, CoGNNs maintains consistent superiority in LUT and BRAM metrics, exhibiting an average prediction error reduction of 44.57% and 23.64% compared to alternative models.

As shown in Table 3, CoGNNs(β, α) also exhibits exceptional prediction capabilities compared to SOTA. Compared to GNN-DSE, HGP+SAGE+GF, IronMan-Pro, PNA-R, and PowerGear, the reduction rates of RMSE values are 47.69%, 36.32%, 52.51%, 26.07%, and 25.80% of those of the respective baseline models. This superior performance stems from CoGNNs’ task-specific feature adaptation, as highlighted in its design. All other CoGNNs combinations outperform the baseline models except IronMan-Pro and GNN-DSE. This not only underscores CoGNNs’ transferability, but also demonstrates its ability to dynamically reconfigure the computational graph topology based on task objectives, enabling more effective feature extraction and improved prediction accuracy. Unlike traditional MPNNs, which focus primarily on minimizing loss during training, CoGNNs prioritizes the extraction of graph-level and node-level features to achieve task objectives, with loss reduction being a natural consequence of this process. As evidenced by Figure 6, CoGNN

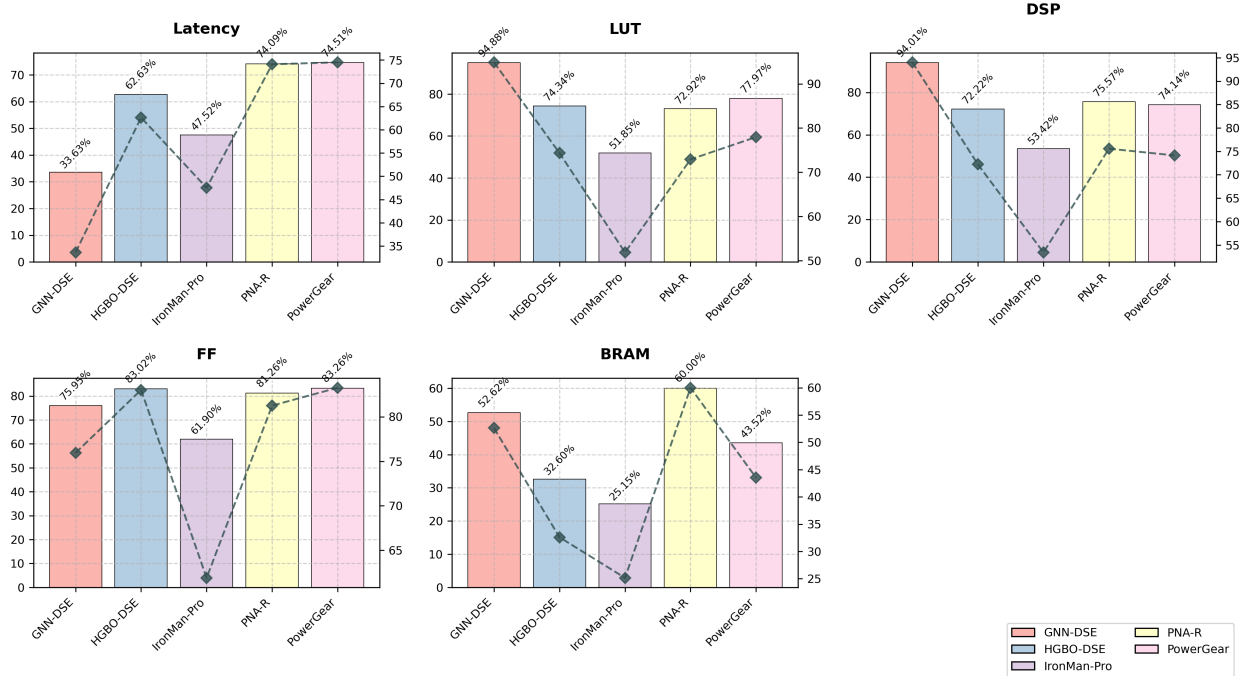


Figure 6: Reduction rates of RMSE loss achieved by CoGNNs(β, α) over baseline models.

Table 4: The benchmarks used for post-implementation QoR prediction.

Kernel name	Description	# Func	# Array	# Loop	# Params
<i>aes</i>	a common block cipher	12	2	11	30
<i>bfs-bulk</i>	Data-oriented version of breadth-first search	1	4	3	25
<i>fft-strided</i>	Recursive formulation of the Fast Fourier Transform	1	4	2	27
<i>gemv-ncubed</i>	O(n ³) algorithm for dense matrix multiplication.	1	3	3	27
<i>md-knn</i>	n-body molecular dynamics, using k-nearest neighbors to compute only local forces	1	7	2	42
<i>nw</i>	A dynamic programming algorithm for optimal sequence alignment	1	6	7	54
<i>sort-radix</i>	Sorts an integer array by comparing 4-bits blocks at a time	7	4	11	72
<i>spmv-ellpack</i>	Sparse matrix-vector multiplication, using fixed-size neighbor lists	1	4	2	25
<i>stencil3d</i>	A three-dimensional stencil computation	1	2	9	43
<i>viterbi</i>	A dynamic programming method for computing probabilities on a Hidden Markov model	1	6	7	52

architectures demonstrate statistically significant improvements over benchmark baseline models. The CoGNN(β, α) variant exhibits superior performance across all evaluation metrics, particularly achieving at least 33.63% RMSE reduction in latency measurements. With particular strength in hardware utilization metrics, the framework achieves peak error reduction of 94.01% for DSP and mean error reductions of 74.44% (LUT), 77.08% (FF), and 42.78% (BRAM) respectively, outperforming existing approaches in FPGA resource estimation accuracy.

In this experiment, the combination of CoGNNs components significantly influences prediction accuracy. We observe that when the environment and action networks utilize simpler MPNNs like SUMGNN and MEANGNN, prediction errors are substantially lower compared to using more complex models such as GCN. This phenomenon is fundamentally tied to CoGNNs’ operational mechanism(it dynamically selects graph topologies to regulate message flow between nodes). In contrast, complex MPNNs like GCN inherently prioritize the importance of information from neighboring nodes, which contradicts CoGNNs’ design philosophy. CoGNNs autonomously learns which neighbors’ information is relevant for each node, effectively disregarding messages from unimportant neighbors. Consequently, integrating MPNNs like GCN, which predefine neighbor importance, results in suboptimal performance within the CoGNNs framework.

5.3 Evaluation of Post-Implementation QoR Prediction Accuracy

To further validate the accuracy of the proposed CoGNNs, we also evaluate its performance on post-implementation QoR prediction. For LUT, FF, CP and POWER, we employ MAPE as the loss function. For DSP and BRAM where

Table 5: MAPE and MAE of CoGNN(β, α) and SOTA models on unseen applications.

Model	MAPE(%)				MAE	
	LUT	FF	CP	POWER	DSP	BRAM
HGP+SAGE+GF[15]	9.05	9.87	9.87	13.60	1.4282	0.1606
IronMan-Pro[20]	7.35	6.30	10.98	16.34	0.6198	0.1917
PowerGear[14]	-	-	-	11.61	-	-
PNA-R[12]	6.40	6.52	14.03	-	-	-
CoGNNs(β, α)	6.82	5.98	7.54	10.01	0.5339	0.1035

zero-value occurrences exist, we adopt MAE to avoid division-by-zero errors during model optimization. The HGBO-DSE dataset provides labels for LUT, DSP, FF, BRAM, CP and POWER, all extracted from implementation reports. In this experiment, we compare the MAPE and MAE of CoGNNs(β, α) on the GNN-DSE dataset against baseline models including HGP+SAGE+GF, IronMan-Pro, PowerGear and PNA-R. Notably, the HGBO-DSE dataset has a node feature dimension of 15, significantly smaller than the GNN-DSE dataset’s 153-dimensional features. To account for this, we reduce the number of iterations, while ensuring that each model undergoes at least 250 training epochs. It is worth noting that HGBO-DSE’s work does not address and evaluate the model generalization, including for all the reproduced baseline models. In this experiment, we partition the dataset into two subsets comprising 10 applications. As shown in Table 4, six applications (*aes*, *bfs*, *fft*, *gemm*, *md*, *nw*) are used for training, while the remaining applications are reserved as unseen applications for inference.

As shown in Table 5, it can be observed that CoGNNs(β, α) achieves the smallest prediction errors for FF, CP, POWER, DSP, and BRAM compared to baseline models, with values of 5.98%, 7.54%, and 10.01% in terms of MAPE, 0.5339 and 0.1033 in terms of MAE, respectively. For LUT prediction, PNA-R exhibits the lowest error at 6.40, while CoGNNs(β, α) closely follows with 6.82, demonstrating a marginal difference. Notably, in POWER prediction, CoGNNs(β, α) reduces the error to 10.01%, outperforming PowerGear, a model specifically designed for power prediction, which achieves 11.61%. The performance of HGP+SAGE+GF on unseen applications underscores that complex model architectures or mere structural stacking cannot enhance performance in HLS or implementation prediction tasks. In summary, the task-adaptive CoGNN demonstrates exceptional performance in predicting post-place-and-route resource usage and exhibits strong generalization capabilities.

In general, as can be seen from Section 5.2 and Section 5.3, CoGNNs(β, α) achieves the best prediction performance on these two datasets. Facts have proven that in the post-HLS QoR prediction and the post-implementation QoR prediction, complex model structures like PNA-R may not yield excellent prediction results. The key lies in improving the model structure according to the task objectives and extracting high-dimensional features from the CDFG, which can lead to better prediction performance.

5.4 Evaluation of Design Space Exploration

In the DSE experiment, we applied our proposed LLMEA method to explore five unseen applications (*atax*, *bicg*, *doitgen*, *gesummv*, and *mvt*) that were excluded from the training phase, utilizing the CoGNNs(β, α) model trained in Section 5.3 as the evaluator. For each application, the design configurations encompass all possible combinations of the pragma values and the C/C++ code. We implemented a Python-based explorer to convert these configurations into graph data via LLVM and ProGraML, enabling input into the prediction model. The evaluation results are stored, and the top-ranked configurations are identified through iterative refinement. The primary objective of DSE is to identify the Pareto-optimal configuration set. To quantify the quality of the approximate Pareto-optimal set, we employ the average distance from the reference set (ADRS) metric [1]:

$$ADRS(\Gamma, \Omega) = \frac{1}{|\Gamma|} \sum_{\lambda \in \Gamma} \min_{\mu \in \Omega} f(\lambda, \mu) \quad (9)$$

where Γ represents the reference Pareto-optimal set, Ω denotes the approximate Pareto-optimal set, and the function f computes the distance between λ and μ . A lower ADRS value indicates a higher accuracy of the approximate Pareto-optimal set relative to the reference. To assess the performance of LLMEA, we compare it with two classic heuristic algorithms: simulated annealing (SA) [12] and genetic algorithm (GA) [9], as referenced in [17]. The reference Pareto-optimal set is collected from the results generated by the exhaustive DSE algorithm proposed in [28]. To ensure fair comparison of algorithm performance, the parameter configurations for SA, GA, and LLMEA maintain unified settings: both population size N and maximal iterations N_{se} are set to identical values across all algorithms.

Table 6: The unseen applications and the number of design configurations used in DSE.

Benchmark	Description	# Pragmas	# Design configs
<i>atax</i>	Matrix Transpose and Vector Multiplication	5	3,354
<i>bicg</i>	BiCG Sub Kernel of BiCGStab Linear Solver	5	2,975
<i>doitgen</i>	Multi-resolution analysis kernel (MADNESS)	6	179
<i>gesummv</i>	Scalar, Vector and Matrix Multiplication	4	1,581
<i>mvt</i>	Matrix Vector Product and Transpose	8	3,059,001

Table 7: ADRS Results on Unseen Applications.

Algorithm	<i>atax</i>	<i>bicg</i>	<i>doitgen</i>	<i>gesummv</i>	<i>mvt</i>	AVG
SA	0.0321	0.0659	0.0943	0.2297	0.1719	0.1188
GA	0.0831	0.0391	0.1696	0.0617	0.0917	0.0891
LLMEA(deepseek-r1)	0.0107	0.0079	0.0187	0.0170	0.0081	0.0125
LLMEA(deepseek-v3)	0.0458	0.0567	0.0921	0.0763	0.0663	0.0674
LLMEA(GPT-4o)	0.0186	0.0048	0.0146	0.0409	0.0861	0.0329
LLMEA(GPT-4)	0.0131	0.0150	0.0219	0.0277	0.0782	0.0312
LLMEA(GPT-3.5-turbo)	0.0227	0.0055	0.0987	0.0455	0.0498	0.0484
LLMEA(GPT-3.5-instruct)	0.0879	0.0046	0.0106	0.0650	0.0084	0.0353
LLMEA(Qwen2.5)	0.0157	0.0125	0.0302	0.2357	0.0302	0.0648
LLMEA(Qwen-max)	0.0101	0.0095	0.2601	0.0172	0.0793	0.0752
LLMEA(deepseek-r1) Improv. over SA				89.49%		
LLMEA(deepseek-r1) Improv. over GA				85.97%		

Additionally, due to the excessively large design space sizes of certain benchmarks such as *mvt*, we have imposed a one-hour exploration time limit for each benchmark. The adaptive parameter scheme is dynamically adjusted based on the design space size S as follows:

$$(N_{se}, N) = \begin{cases} (0.0005S, 50) & S > 10^6 \\ (0.1S, 30) & 500 < S \leq 10^6 \\ (0.3S, 10) & S \leq 500 \end{cases} \quad (10)$$

Table 6 briefly describes the number of pragmas and the number of design configurations for the five unseen applications. To compare the performance of different LLMs in LLMEA, we adopted nine LLMs, namely deepseek-r1 and deepseek-v3, GPT-4o, GPT-4, GPT-3.5-turbo, GPT-3.5-instruct, Qwen2.5, Qwen-max as the models for our experiment, and compared them with the two classic heuristic algorithms, SA and GA. The ADRS results achieved by LLMEAs, SA and GA are shown in Table 7. In more details, for the *atax* application, LLMEA(Qwen-max) achieves the lowest average ADRS of 0.0125, representing improvements of 68.68% and 87.88% over SA and GA, respectively. For the *bicg* and *doitgen* kernels, LLMEA(GPT-3.5-instruct) demonstrates significant accuracy enhancements of 93.08%, 88.34% and 88.79%, 93.77% compared to SA and GA. Notably, LLMEA(deepseek-r1) delivers the best performance in the *gesummv* and *mvt* applications, as well as in overall accuracy. Specifically, LLMEA(deepseek-r1) improves overall accuracy by 89.49% and 85.97% over SA and GA, respectively. Fig 7 compares the convergence curves of the top-performing LLMEAs with GA and EA across five benchmarks. The results demonstrate that LLMEAs achieve both faster convergence rates and higher-quality solutions than traditional heuristic algorithms. Notably, LLMEAs exhibit superior optimization capabilities when exploring equivalent design configurations: they outperform baseline methods in both compact design spaces (e.g., *doitgen*, *gesummv*) and extremely large-scale design spaces (e.g., *mvt*), showing enhanced resistance to local optima stagnation.

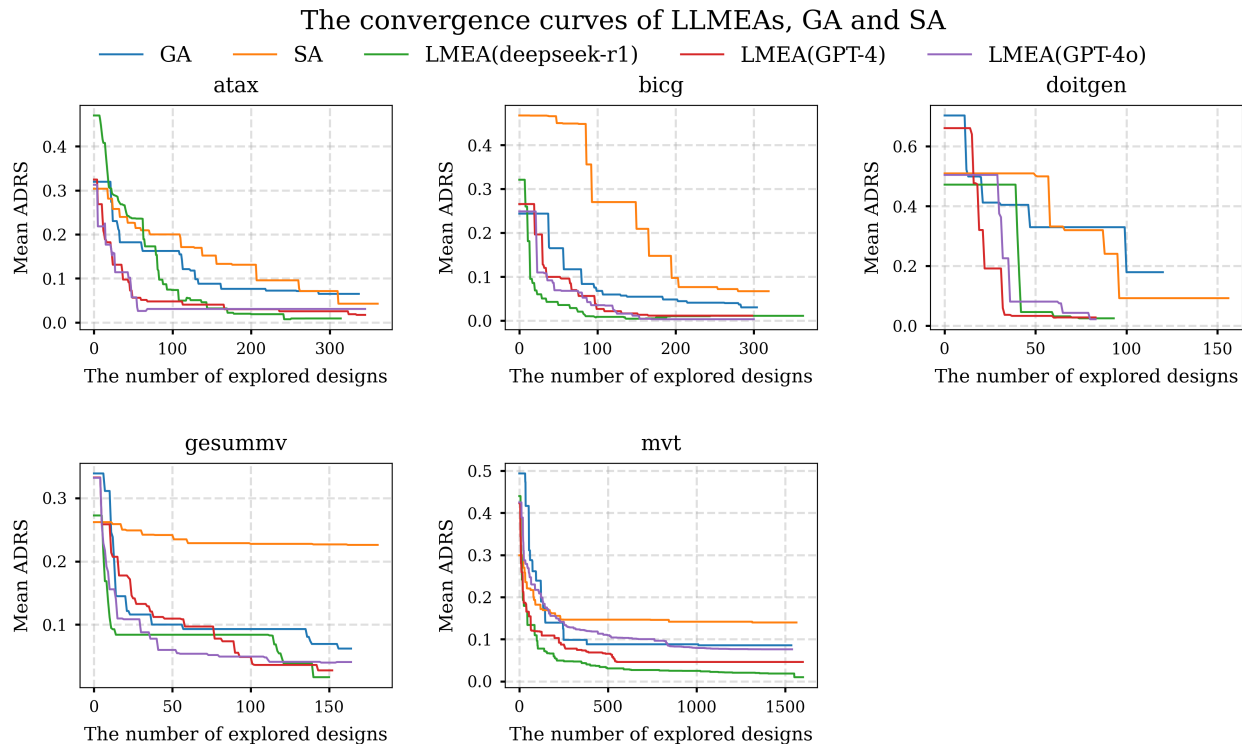


Figure 7: Convergence Curves: Mean ADRS achieved by LLMEAs, SA and GA as the number of explored designs increases.

6 Conclusion

In this paper, we present the CoGNNs-LLMEA framework, which comprises a GNN prediction model that dynamically adapts message-passing strategies based on task-specific characteristics and an LLM-driven evolutionary algorithm for DSE. CoGNNs enhances LLMEA’s exploration capabilities by providing high-precision QoR predictions for design configurations without relying on time-consuming EDA flows. Experimental results demonstrate that both CoGNNs and LLMEA outperform baseline models across multiple metrics. This work presents the first systematic implementation of LLMs in DSE. Beyond demonstrating LLMs’ capability to autonomously execute complex crossover and mutation operations traditionally requiring human expertise, we aim to address the limitations of conventional heuristic-based methodologies that dominate current DSE practices. More significantly, our LLMEA framework demonstrates superior performance compared to traditional heuristic approaches. The proposed paradigm shift of leveraging LLMs for domain-specific knowledge-intensive tasks establishes a new methodology with promising potential for widespread adoption in DSE research and applications. The current implementation of LLMEA presents valuable opportunities for enhancement in future endeavors. By addressing specific areas for improvement, we can significantly elevate its effectiveness and impact.

- 1) **Improving the selection of LLMs** The current DSE experiment implemented multiple LLMs, though the investigation does not comprehensively encompass all established model archetypes. Notably, the hypothesis that LLMs specifically designed for mathematical reasoning and code generation might demonstrate superior configuration generation capabilities compared to conversational LLMs in DSE contexts remains to be rigorously validated through systematic comparative analysis.
- 2) **Reducing the runtime of LLMEA** In the experiments, we employed multiple LLMs, necessitating the implementation of Langchain for online LLM orchestration. However, most LLMs (particularly deepseek-r1) were observed to require extended inference latency, resulting in a prolonged experimental execution duration. A potential mitigation strategy involves conducting cloud-based LLM performance benchmarking to identify optimal candidates, followed by localized deployment of selected models to reduce API-dependent computational overhead.
- 3) **Optimizing prompt engineering techniques** Experimental results empirically demonstrate that the output quality of LLMs exhibits strong dependency on prompt configuration design. Dedicated prompt engineering

techniques, such as self-reflective prompts [35] and directional-stimulus prompts [36], may lead to more significant performance enhancements in LLMEA’s evolutionary optimization processes.

References

- [1] Benjamin Carrion Schafer and Zi Wang. High-level synthesis design space exploration: Past, present, and future. *IEEE Transactions on Computer-Aided Design of Integrated Circuits and Systems*, 39(10):2628–2639, 2019.
- [2] Ben Finkelshtein, Xingyue Huang, Michael Bronstein, and Ceylan. Cooperative graph neural networks. In *Proceedings of the 41st International Conference on Machine Learning, ICML’24*. JMLR.org, 2024.
- [3] Keyulu Xu, Weihua Hu, Jure Leskovec, and Stefanie Jegelka. How powerful are graph neural networks? *arXiv preprint arXiv:1810.00826*, 2018.
- [4] Vijay Prakash Dwivedi, Ladislav Rampásek, Michael Galkin, Ali Parviz, Guy Wolf, Anh Tuan Luu, and Dominique Beaini. Long range graph benchmark. *Advances in Neural Information Processing Systems*, 35:22326–22340, 2022.
- [5] Qimai Li, Zhichao Han, and Xiao-Ming Wu. Deeper insights into graph convolutional networks for semi-supervised learning. In *Proceedings of the AAAI conference on artificial intelligence*, volume 32, 2018.
- [6] Petar Veličković, Guillem Cucurull, Arantxa Casanova, Adriana Romero, Pietro Lio, and Yoshua Bengio. Graph attention networks. *arXiv preprint arXiv:1710.10903*, 2017.
- [7] Steve Dai, Yuan Zhou, Hang Zhang, Ecenur Ustun, Evangeline FY Young, and Zhiru Zhang. Fast and accurate estimation of quality of results in high-level synthesis with machine learning. In *2018 IEEE 26th Annual International Symposium on Field-Programmable Custom Computing Machines (FCCM)*, pages 129–132. IEEE, 2018.
- [8] Guanwen Zhong, Alok Prakash, Siqi Wang, Yun Liang, Tulika Mitra, and Smail Niar. Design space exploration of fpga-based accelerators with multi-level parallelism. In *Design, Automation & Test in Europe Conference & Exhibition (DATE), 2017*, pages 1141–1146. IEEE, 2017.
- [9] Hosein Mohammadi Makrani, Farnoud Farahmand, Hossein Sayadi, Sara Bondi, Sai Manoj Pudukotai Dinakarrao, Houman Homayoun, and Setareh Rafatirad. Pyramid: Machine learning framework to estimate the optimal timing and resource usage of a high-level synthesis design. In *2019 29th International Conference on Field Programmable Logic and Applications (FPL)*, pages 397–403. IEEE, 2019.
- [10] Lorenzo Ferretti, Andrea Cini, Georgios Zacharopoulos, Cesare Alippi, and Laura Pozzi. Graph neural networks for high-level synthesis design space exploration. *ACM Transactions on Design Automation of Electronic Systems*, 28(2):1–20, 2022.
- [11] Mingzhe Gao, Jieru Zhao, Zhe Lin, and Minyi Guo. Hierarchical source-to-post-route qor prediction in high-level synthesis with gnns. In *2024 Design, Automation & Test in Europe Conference & Exhibition (DATE)*, pages 1–6. IEEE, 2024.
- [12] Nan Wu, Hang Yang, Yuan Xie, Pan Li, and Cong Hao. High-level synthesis performance prediction using gnns: Benchmarking, modeling, and advancing. In *Proceedings of the 59th ACM/IEEE Design Automation Conference*, pages 49–54, 2022.
- [13] Chenfeng Zhao, Clayton Faber, Roger Chamberlain, and Xuan Zhang. Hlperf: demystifying the performance of hls-based graph neural networks with dataflow architectures. *ACM transactions on reconfigurable technology and systems*, 18(1):1–26, 2024.
- [14] Zhe Lin, Zike Yuan, Jieru Zhao, Wei Zhang, Hui Wang, and Yonghong Tian. Powergear: Early-stage power estimation in fpga hls via heterogeneous edge-centric gnns. in *2022 design, automation & test in europe conference & exhibition (date)*. *IEEE, Virtual*, pages 1341–1346, 2022.
- [15] Huizhen Kuang, Xianfeng Cao, Jingyuan Li, and Lingli Wang. Hgbo-dse: Hierarchical gnn and bayesian optimization based hls design space exploration. In *2023 International Conference on Field Programmable Technology (ICFPT)*, pages 106–114. IEEE, 2023.
- [16] Atefeh Sohrabzadeh, Yunsheng Bai, Yizhou Sun, and Jason Cong. Harnessing gnns for robust representation learning in high-level synthesis. *IEEE Transactions on Circuits and Systems for Artificial Intelligence*, 1(2):114–127, 2024.
- [17] Zi Wang and Benjamin Carrion Schafer. Machine learning to set meta-heuristic specific parameters for high-level synthesis design space exploration. in *2020 57th acm/ieee design automation conference (dac)*. 1–6, 2020.

- [18] Pingakshya Goswami, Benjamin Carrion Schaefer, and Dinesh Bhatia. Machine learning based fast and accurate high level synthesis design space exploration: From graph to synthesis. *Integration*, 88:116–124, 2023.
- [19] Huiliang Hong, Chenglong Xiao, and Shanshan Wang. Rethinking high-level synthesis design space exploration from a contrastive perspective. In *2024 IEEE 42nd International Conference on Computer Design (ICCD)*, pages 179–182. IEEE, 2024.
- [20] Nan Wu, Yuan Xie, and Cong Hao. Ironman-pro: Multiobjective design space exploration in hls via reinforcement learning and graph neural network-based modeling. *IEEE Transactions on Computer-Aided Design of Integrated Circuits and Systems*, 42(3):900–913, 2023.
- [21] Yuan Yao, Huiliang Hong, Shanshan Wang, and Chenglong Xiao. Decomposition based estimation of distribution algorithm for high-level synthesis design space exploration. *Integration*, 100:102292, 2025.
- [22] Md Imtiaz Rashid and Benjamin Carrion Schaefer. Fast and inexpensive high-level synthesis design space exploration: Machine learning to the rescue. *IEEE Transactions on Computer-Aided Design of Integrated Circuits and Systems*, 42(11):3939–3950, 2023.
- [23] Zheyuan Zou, Cheng Tang, Lei Gong, Chao Wang, and Xuehai Zhou. Flexwalker: An efficient multi-objective design space exploration framework for hls design. In *2024 34th International Conference on Field-Programmable Logic and Applications (FPL)*, pages 126–132, 2024.
- [24] Thomas N Kipf and Max Welling. Semi-supervised classification with graph convolutional networks. *arXiv preprint arXiv:1609.02907*, 2016.
- [25] Chris Lattner and Vikram Adve. Llvm: A compilation framework for lifelong program analysis & transformation. In *International symposium on code generation and optimization, 2004. CGO 2004.*, pages 75–86. IEEE, 2004.
- [26] Chris Cummins, Zacharias V Fisches, Tal Ben-Nun, Torsten Hoefler, Michael FP O’Boyle, and Hugh Leather. Programl: A graph-based program representation for data flow analysis and compiler optimizations. In *International Conference on Machine Learning*, pages 2244–2253. PMLR, 2021.
- [27] Eric Jang, Shixiang Gu, and Ben Poole. Categorical reparameterization with gumbel-softmax. *arXiv preprint arXiv:1611.01144*, 2016.
- [28] Atefeh Sohrabzadeh, Yunsheng Bai, Yizhou Sun, and Jason Cong. Automated accelerator optimization aided by graph neural networks. In *Proceedings of the 59th ACM/IEEE Design Automation Conference, DAC ’22*, page 55–60, 2022.
- [29] Yujia Li, Daniel Tarlow, Marc Brockschmidt, and Richard Zemel. Gated graph sequence neural networks. *arXiv preprint arXiv:1511.05493*, 2015.
- [30] Shengcai Liu, Caishun Chen, Xinghua Qu, Ke Tang, and Yew-Soon Ong. Large language models as evolutionary optimizers. In *2024 IEEE Congress on Evolutionary Computation (CEC)*, pages 1–8. IEEE, 2024.
- [31] Elliot Meyerson, Mark J Nelson, Herbie Bradley, Adam Gaier, Arash Moradi, Amy K Hoover, and Joel Lehman. Language model crossover: Variation through few-shot prompting. *ACM Transactions on Evolutionary Learning*, 4(4):1–40, 2024.
- [32] Brandon Reagen, Robert Adolf, Yakun Sophia Shao, Gu-Yeon Wei, and David Brooks. Machsuite: Benchmarks for accelerator design and customized architectures. In *2014 IEEE International Symposium on Workload Characterization (IISWC)*, pages 110–119. IEEE, 2014.
- [33] T. Yuki et al. Polybenchc, 4.2.1, 2010. <https://github.com/MatthiasJReisinger/PolyBenchC-4.2.1>.
- [34] William L Hamilton. *Graph representation learning*. Morgan & Claypool Publishers, 2020.
- [35] Noah Shinn, Federico Cassano, Ashwin Gopinath, Karthik Narasimhan, and Shunyu Yao. Reflexion: language agents with verbal reinforcement learning. In A. Oh, T. Naumann, A. Globerson, K. Saenko, M. Hardt, and S. Levine, editors, *Advances in Neural Information Processing Systems*, volume 36, pages 8634–8652. Curran Associates, Inc., 2023.
- [36] Zekun Li, Baolin Peng, Pengcheng He, Michel Galley, Jianfeng Gao, and Xifeng Yan. Guiding large language models via directional stimulus prompting. NIPS ’23, Red Hook, NY, USA, 2023. Curran Associates Inc.